CrossMark

ORIGINAL ARTICLE

Biosynthesis of MgO nanoparticles using mushroom extract: effect on peanut (*Arachis hypogaea L.*) seed germination

K. Jhansi[1] · N. Jayarambabu[2] · K. Paul Reddy[2] · N. Manohar Reddy[3] · R. Padma Suvarna[1] · K. Venkateswara Rao[4] · V. Ramesh Kumar[5] · V. Rajendar[6]

Abstract Current study describes the green, environmental friendly, and cost-effectiveness technique for the preparation of MgO nanoparticles (NPs) via white button mushroom aqueous extract. The synthesized MgO NPs were characterized using equipments such as X-ray diffraction, dynamic light scattering (DLS), scanning electron microscope (SEM), energy dispersive spectroscopy (EDS), and thermal gravimetric analysis (TGA) for average crystalline size, particle size, morphology, elemental analysis, and weight loss of the materials, respectively. This study reports the application of gardened sizes of (20, 18.5, 18, 16.5, and 15 nm) biosynthesized MgO NPs on seed germination. The smaller size (15 nm) MgO NPs have been enhanced the seed germination and growth parameters as compared with remaining sizes of MgO NPs and control. The magnesium oxide NPs penetrates into peanut seeds and affecting on seed germination and growth rate mechanism. In addition, this germination found to be high in seeds than germination on selected soil plot MgO NPs (0.5 mg/L stable concentrations) compared to different size of MgO NPs and control. Physicochemical methods indicated that the MgO NPs are able to penetrate into the seed coat and support water uptake inside of seeds. Probably, this positive effect may cause for the uptake of MgO NPs by the plants, as indicated in the UV and SEM analyses. As the smaller size (15 nm) of MgO NPs particles stimulates the development of seedling and growth enhancement of peanut, it clearly indicates that the current study is helpful in growing of peanuts in large-scale agricultural production.

✉ N. Manohar Reddy
  manoharreddy123n@gmail.com

✉ V. Rajendar
  rajendar.nano@gmail.com

1 Department of Physics, Jawaharlal Nehru Technological University Ananthapur, Ananthapur, Andhra Pradesh 515001, India

2 Centre for Nano Science and Technology, Institute of Science and Technology, Jawaharlal Nehru Technological University Hyderabad, Kukatpally, Hyderabad, Telangana 500085, India

3 Department of Physics, S.V.E College, Tirupati, Andhra Pradesh 515001, India

4 Radiology Department, School of Medicine, Johns Hopkins University, Baltimore, USA

5 Department of Physics, Government Degree College, Pattikonda, Kurnool, Andhra Pradesh 518380, India

6 Department of Electronic Engineering, Yeungnam University, Gyeongsan-Si, Gyeongsangbuk-do 38541, Republic of Korea

Introduction

Nanotechnology is an emerging field which involves the control and construction of improved new material at nanoscale level (Thakkar et al. 2010). Conventionally, chemical precipitation (Panigrahi et al. 2004) and thermal evaporation (Yang et al. 2006) have been reported to employ MgO nanostructures for different particle sizes. These synthesis techniques are sophisticated, constrained by expense equipment, utilization of high temperature, pressure, for production of metal oxides, etc. Moreover,

Springer

MgO NPs prepared by those conservative methods often yield a relative small surface area and hence show low reaction activity (Anthony et al. 2014). Therefore, the biosynthesis of MgO NPs has been attempted in the present study. Microorganisms like bacteria and fungi have naturally bestowed property of reducing and oxidizing metal ions into metallic or metal oxide NPs, thereby functioning as nanofactories (Sadeghi and Hosseini 2012; Matteis et al. 2012; Jaison et al. 2017; Sutradhar et al. 2011). The MgO NPs caused an increase in photosynthesis in peanut which enhances the ability to absorb and utilize light. However, this NPs stimulated antioxidant systems and hastened the germination and growth of plants (Mageshwari et al. 2013). Analyzing the level of penetration and transportation mechanism of NPs in plant growth is key point to apply the nanotechnology to agriculture (Tamilselvi et al. 2013). At present, MgO NPs were utilizing in many commercial products like textiles, detergents, and antimicrobial agents, etc. There are some growing factors about their effect on the environment (plants, animals, and people) (Hayashi and Hakuta 2010; Hou et al. 2003). The present research investigation embodies in biosynthesis of MgO NP and its effect on chlorophyll contents in peanut plant leaves and rapid biosynthesis under laboratory conditions, characterization of MgO NPs and its influence on seed germination, biomass, dry biomass, and chlorophyll content in Peanut plant.

Materials and methods

Preparation of white mushroom extraction

Twenty-five grams of fresh Mushrooms were taken and washed several times with distilled water to remove any organic impurities present in it, and then, the crushed pieces and 250 mL of distilled were taken into the 2 L beaker thoroughly stirred for 30 min followed by filtration process using Whatman filter paper. Here, mushroom extract used as the reducing and stabilizing agent for synthesis of MgO NPs.

Synthesis of magnesium nanoparticles

Above-prepared mushroom extract taken with an aqueous solution of 0.1 M magnesium acetate (Mg (CH$_3$COO)$_2$ 4H$_2$O) solution and kept for 2 h stirring; the temperature maintained at 40 °C. The change of color takes place within 30 min from colorless to light brown color in the presence of magnesium acetate. After that, the mixture transferred on to hot plate to carry out biocombustion process. The resultant products were calcined at 400 °C for 4 h to get MgO NPs.

Results and discussion

X-ray diffraction (XRD) analysis

Figure 1 represents the X-ray diffraction pattern of the magnesium oxide nanoparticles from the biosynthesis method, which were calcinated at 400 °C; it is clearly observed that the highest intensity peak is obtained at 42.93° crystal planes of MgO (111). It shows that crystal structure is cubic with lattice constant of $a = b = c = 0.4291$ nm. The peaks were observed at 36.93°, 42.93°, 62.27°, 74.77°, and 78.69° along with the miller indices (hkl) values (111), (200), (220), (311), and (222) crystal planes (Mirzaei and Davoodnia 2012). These results were matched with JCPDS Card No. 89-7746. The sharp diffraction peaks were clearly seen and they perfectly match with crystal structure of MgO; therefore, we get clear crystallinity of MgO NPs having that the average crystallite size is 20 nm at 10 mL, 18.5 nm at 20 mL, 18 nm at 40 mL, 16.5 nm at 60, mL and 15 nm at 80 mL extractions, Obtained from the Debye–Scherrer equation is the following equation:

$$D = \frac{K \cdot \lambda}{\beta \cos \theta},$$

where D is average crystallite size, K Debye–Scherrer's constant (=0.94), λ CuKα-radiation (0.154 nm), β FWHM of the peak, and θ Bragg's angle.

Particle size analyzer (PSA)

Particle size distribution analysis was done with dynamic light scattering I aqueous solution. From Fig. 2, it was found that the average size of MgO NPs for 10 mL
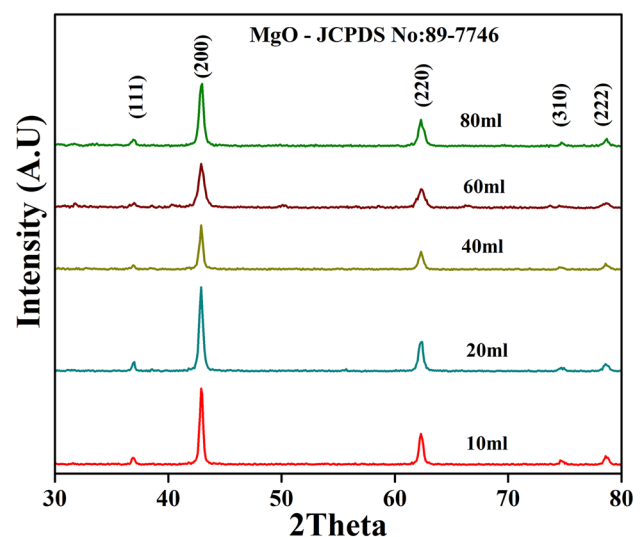

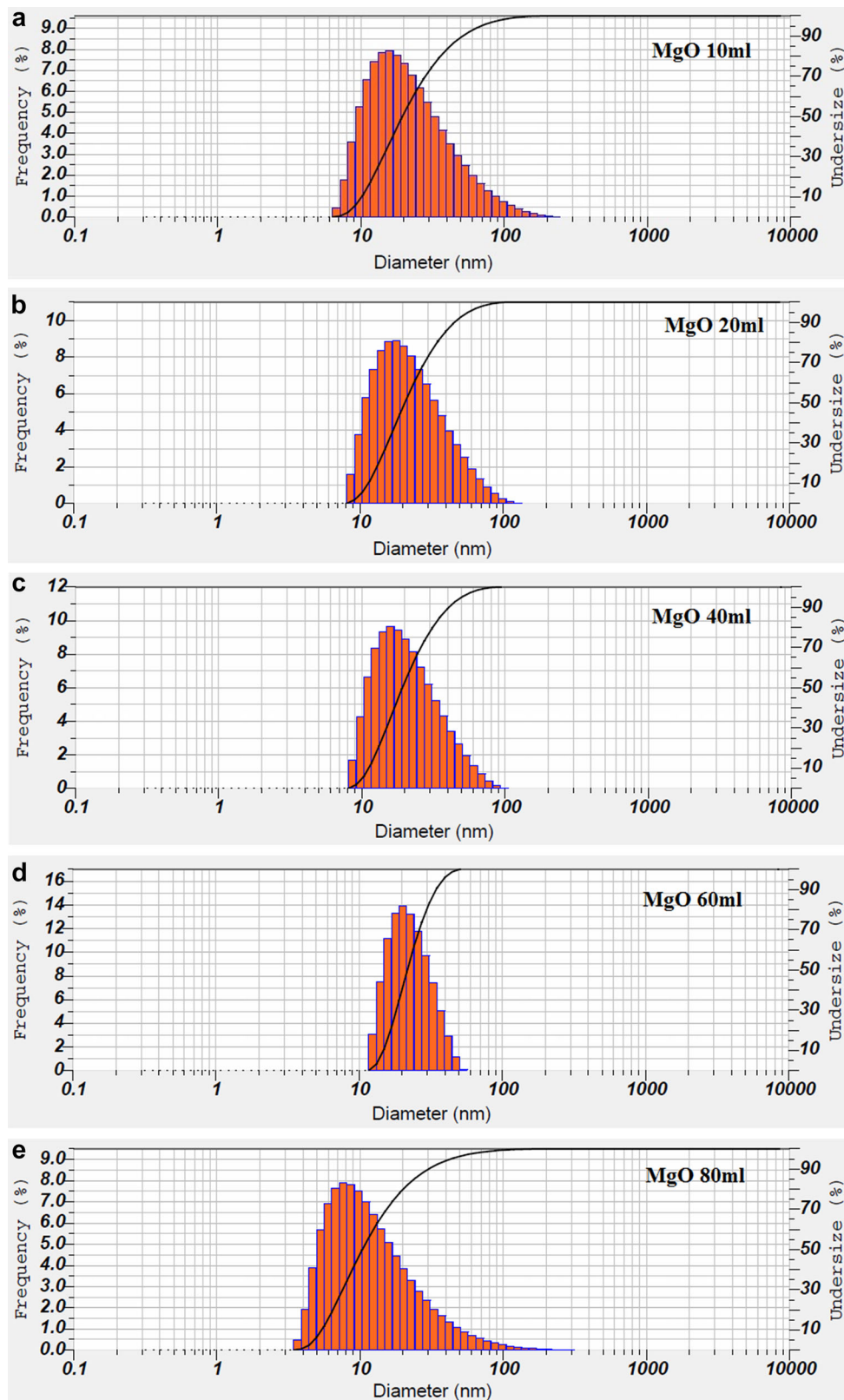**Fig. 1** X-ray diffraction pattern of MgO nanoparticles

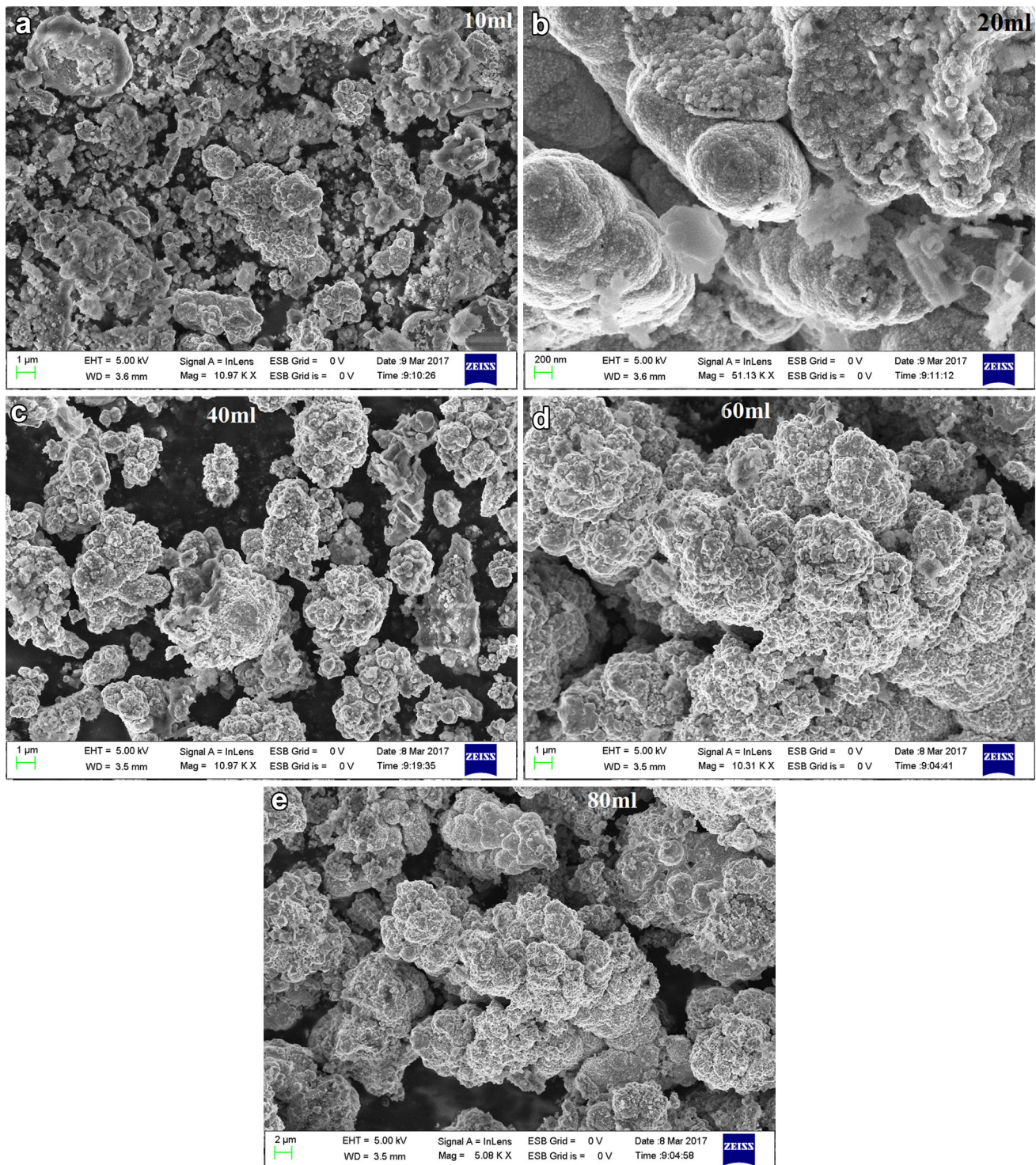**Fig. 2** Particle distribution of different sizes of MgO NPs

Fig. 3 SEM image of different sizes MgO NPs

extract is 38.6 nm, 20, 40, 60, and 80 mL extract is 35.3, 34.1, 32.4 and 29.6 nm, respectively, while increasing the concentrations of extraction solution then the average particle size will be decreasing (Vatsha et al. 2013). These results were incoherence with XRD average crystallite size.

Scanning electron microscope (SEM)

Scanning electron microscopic analysis was employed to study the surface morphology of the MgO NPs that were formed. Representative SEM micrographs of the synthesized NPs carried out at various magnifications are
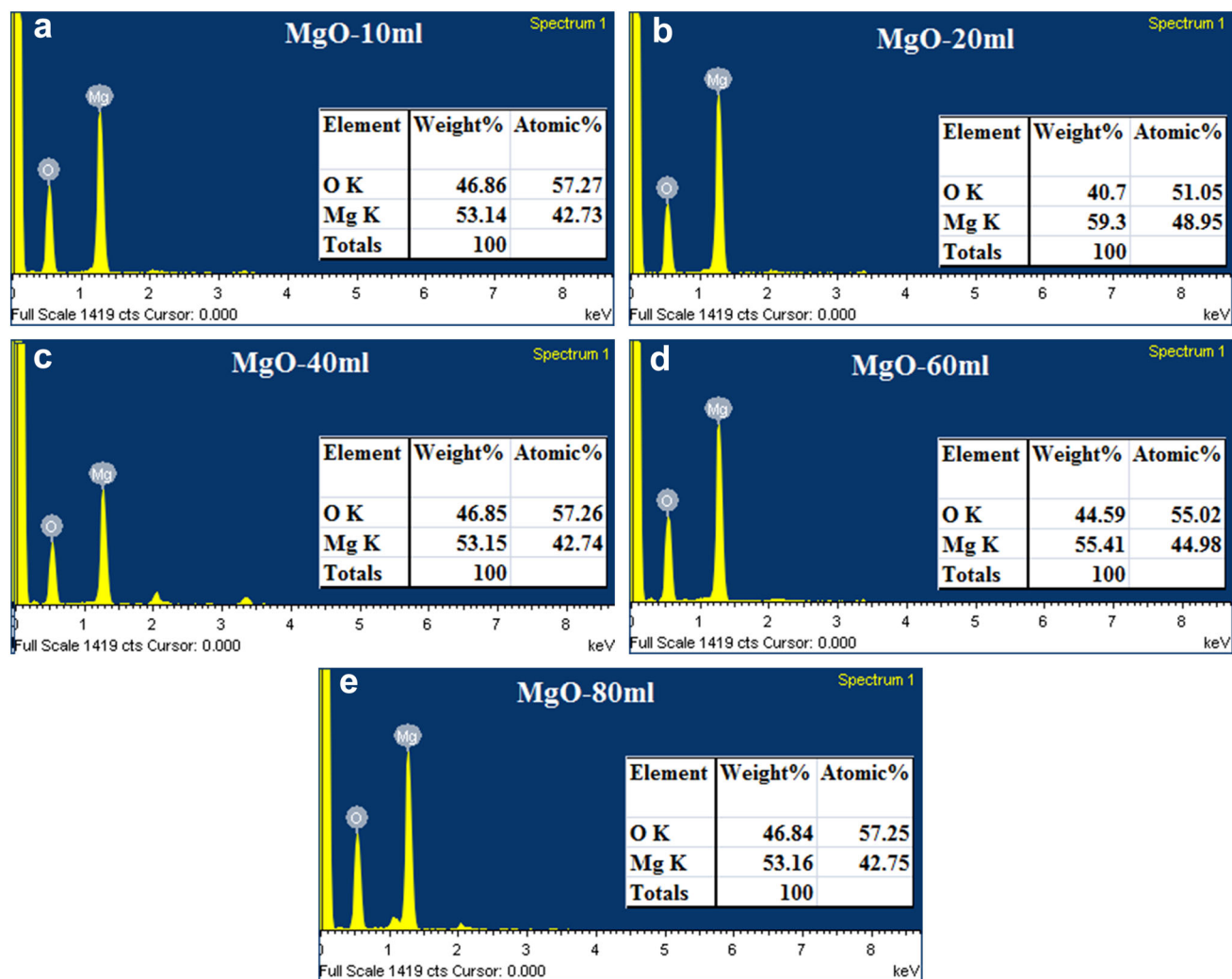
Fig. 4 EDS spectra and elemental composition of MgO NPs

displayed in (Fig. 3), respectively. In the lower magnification SEM image, it can be observed that even though the particles are well distributed, the boundaries between each particle are not clearly examinable, while at the higher magnification images, the surface morphology of granules and monodispersive clusters in the form of assemblies are evidently predictable. Moreover, the boundaries between each particle can be seen. It is also noticed that the particles have agglomerated into clusters because of attractive forces which bringing them together into groups. SEM image shows that the average particle size is 1 μm.

Energy dispersive X-ray analysis (EDS)

Energy dispersive X-ray spectroscopy (EDX) spectrum reveals the presence of Mg and O elements in MgO (Fig. 4)

(Patil and Bhanage 2013). Graph demonstrates the typical EDX result of MgO. It is confirmed from the EDX analysis that the grown NPs are composed of Mg and oxygen only. The molecular ratio of Mg:O of the MgO NPs was found to be 1.2:1(Fig. 4). We did not observe any other peaks of other elements in the spectrum, which confirms again that the grown NPs are pure MgO NPs.

Thermo gravimetric and differential thermal analysis (TG/DTA)

The thermal properties of MgO (10, 20, 40, 60, and 80 mL) have been studied by TGDTA under nitrogen atmosphere at 10 °C/min, as shown in Fig. 5. For all the samples, the thermal decomposition has been observed in the temperature range of 30–395 °C with the exothermic peak around 235–245 °C due to decomposition of carbon and organic
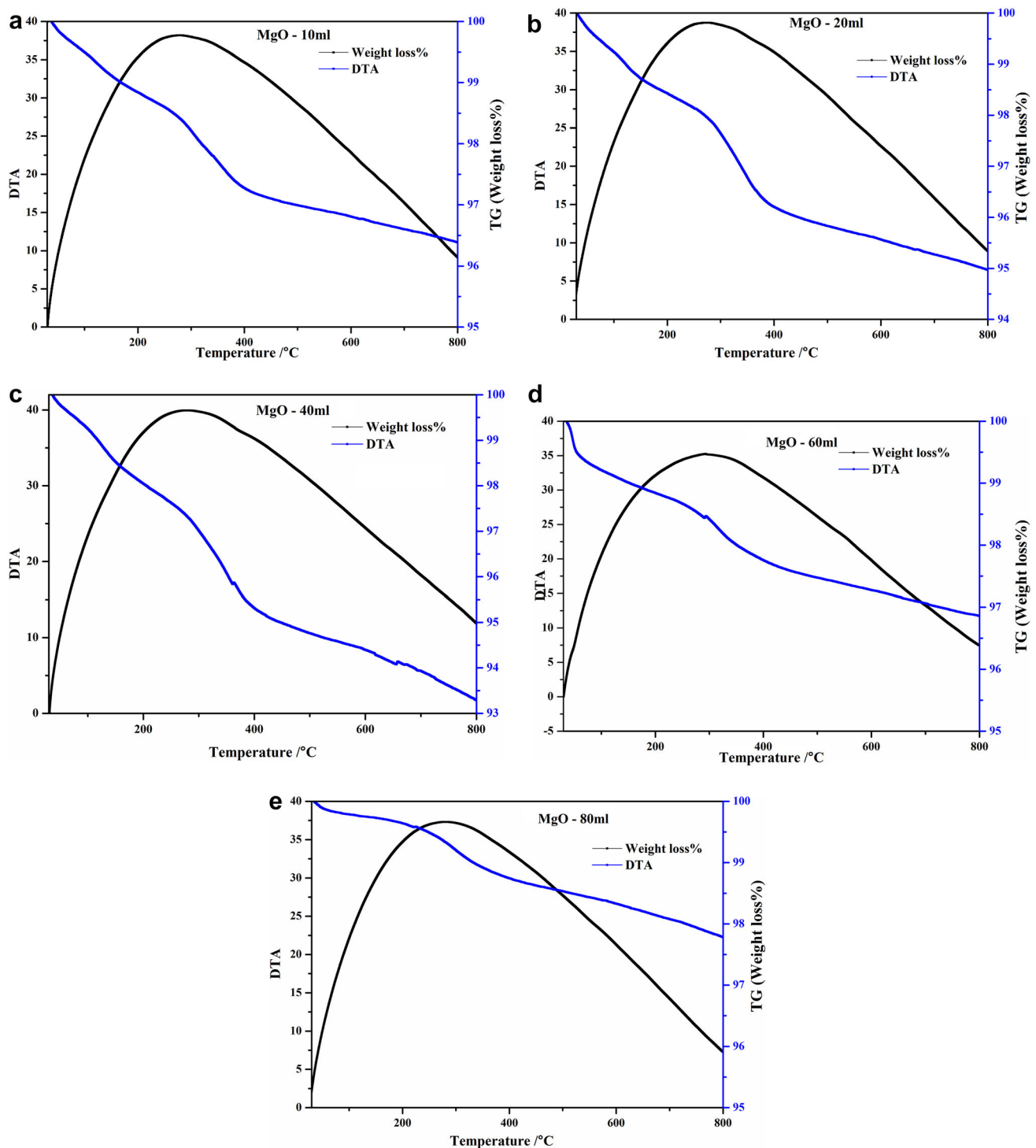
Fig. 5 TG/DTA curves of MgO NPs

compounds. After 400 °C, the weight loss occurs due to the untreated materials which were presented in the sample Ganesan et al. (2013). All the samples weight losses found to be below 5% only (10 mL: 3.8%, 20 mL: 4.6%, 40 mL: 5%, 60 mL: 3.6%, and 80 mL: 4.1%), which indicates stability of crystalline solid phases.

Seed preparation and treatment

To ensure the surface sterility, the seeds were immersed in 10% of sodium hypochlorite (10 min). The MgO NPs were suspended (0.5 mg/L) in deionized water and dispersed by ultrasonic vibration at 100 W, 40 kHz for 30 min. Before use,

small magnetic bars were placed in the suspensions for stirring to avoid aggregation of the particles. Then, the peanut seeds were soaked in deionized water and NP suspensions for about 12 h after the sprouted seeds are being planted on selected soil plot to investigate the effect of NPs on peanut plant growth. After keeping 6 days in the green house under room temperature condition, germination was more than 90% in treated MgO NPs suspensions and control showed that 80% seeds had germinated and developed roots that were at least 30 mm long. Then, the germination was halted, and seed germination percentage and root nodules were calculated. The fresh biomass and dry biomass were measured.

Effect of MgO NPs on seed germination, fresh biomass, dry biomass, and number of root nodules

Figures 6, 7 show the germination percentage, number of root nodules, fresh biomass, and dry biomass of peanut

treated with different sizes of MgO NPs, respectively. Figure 7 confirms the significance of 15 nm-size MgO NPs which causes the increase of fresh and dry biomass. Some what, this outcome is contradictory with the previous study (Zhang et al. 2016), but these results demonstrate that the prepared MgO NPs significantly elevated the dry biomass of peanut with comparative to remaining sizes treatment. We observed higher growth rate of plant in all MgO treatment NPs than control. This confirms that MgO NPs could be an in ideal substitution for agriculture and can be used as Mg source by peanut plants.

Estimation of total chlorophyll content

The concentration of chlorophyll a and b in obtained extracts was measured by Systronics Double Beam UV–Vis Spectrophotometer: 2202. According to these measurements, chlorophyll-a and -b content in fresh materials
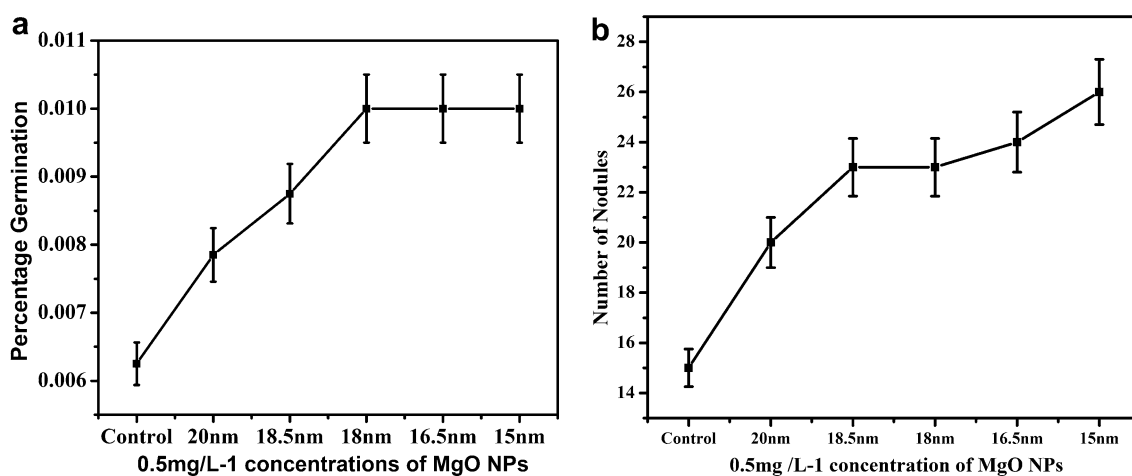

Fig. 6 Effect of MgO NPs of various sizes on seed germination percentage fresh biomass of peanut plant
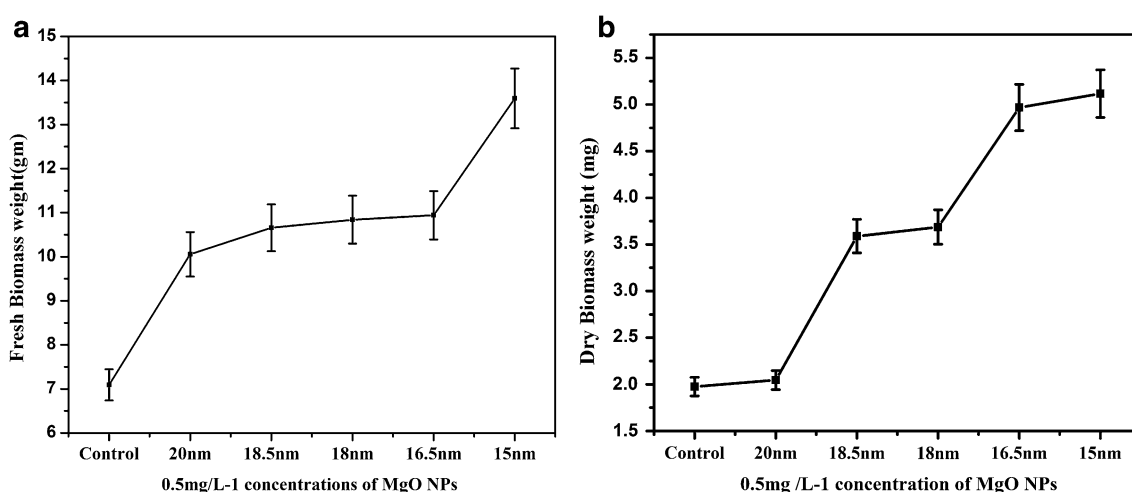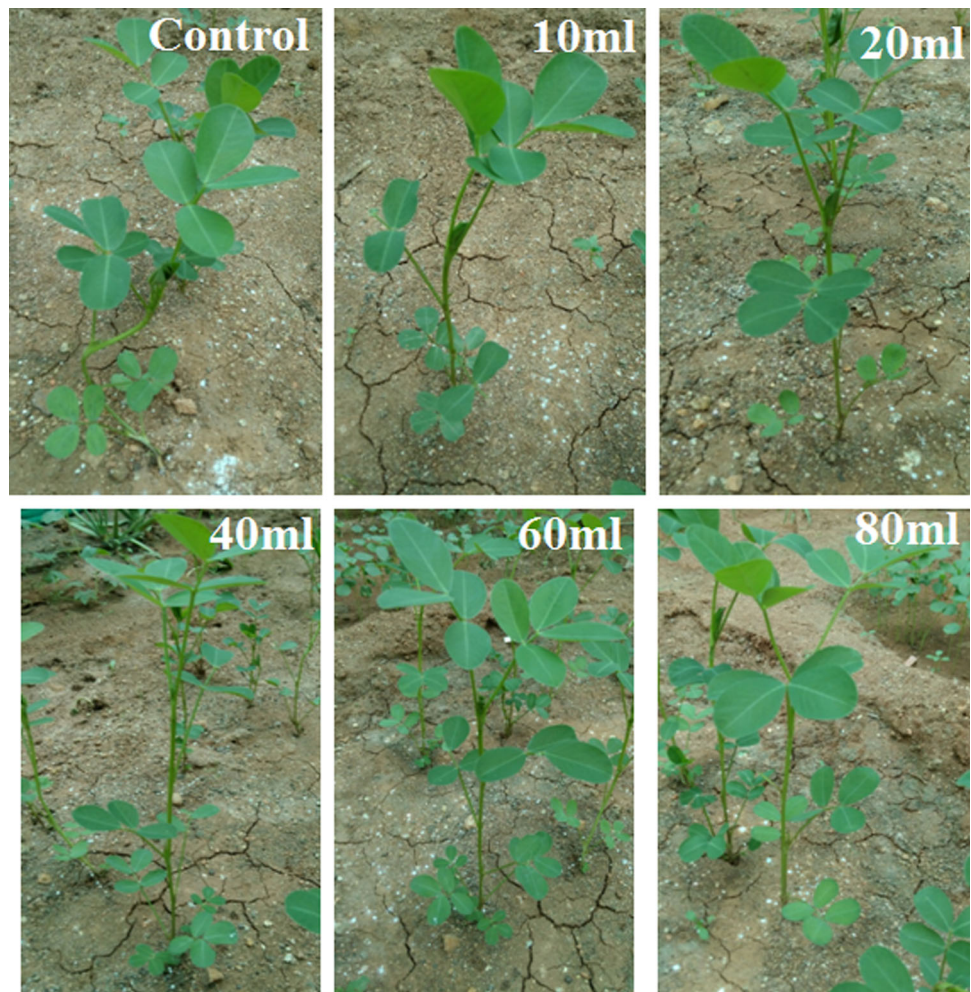

Fig. 7 Biosynthesized MgONPs of various sizes effect on dry biomass and peanut nodules of peanut plant

Fig. 8 Peanut seeds treated by different size of MgO NPs and control

of peanut leaves was shown in (Fig. 8). Chlorophyll plays an important role in the development of assimilating system of plants. Its concentration varies with age and maturity, day length, light intensity of illumination, season, and environment (Saifuddin et al. 2009; Sachin et al. 2012). The obtained results clearly indicate that biosynthesized MgO NPs enhance chlorophyll in the peanut plant leaves. The biologically prepared, functional NPs are financially cheap and environmentally benign. Biologically engineered MgO can be directly used in biomedical, engineering, agricultural, and allied sectors, and it is well supported by the previous research reports (Li et al. 2011; Bar et al. 2009; Ramesh et al. 2014). Results states that there is remarkably increased chlorophyll (photosynthetic pigment) contents. The central metal atom of MgO acts as chlorophyll structure which might be the reason for better response of MgO NPs. The size and surface properties of NPs will affect the uptake phenomena. The NPs could enter the xylem via the cortex and the central cylinder, and may accumulate in the vacuole and are adsorbed on to the plant surface and taken up through natural nanometer or
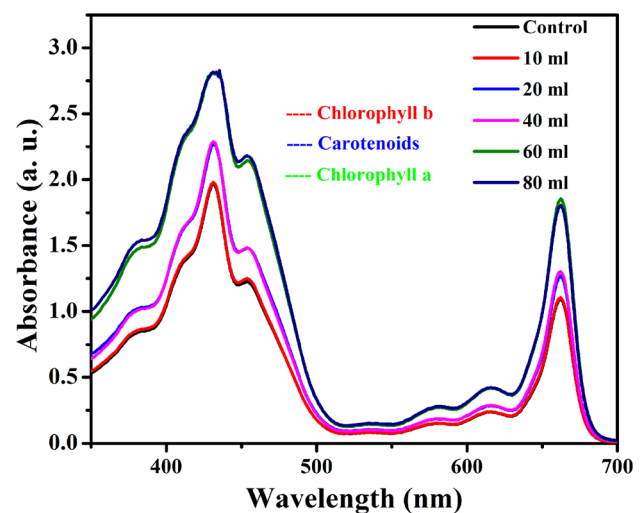

Fig. 9 Effect of the different size of MgO NPs on chlorophyll analysis of peanut plant

micrometer scale plant openings (Sushma et al. 2016). Several pathways exist which are predicted for NP association and uptake in plants. The biosynthesized MgO NPs
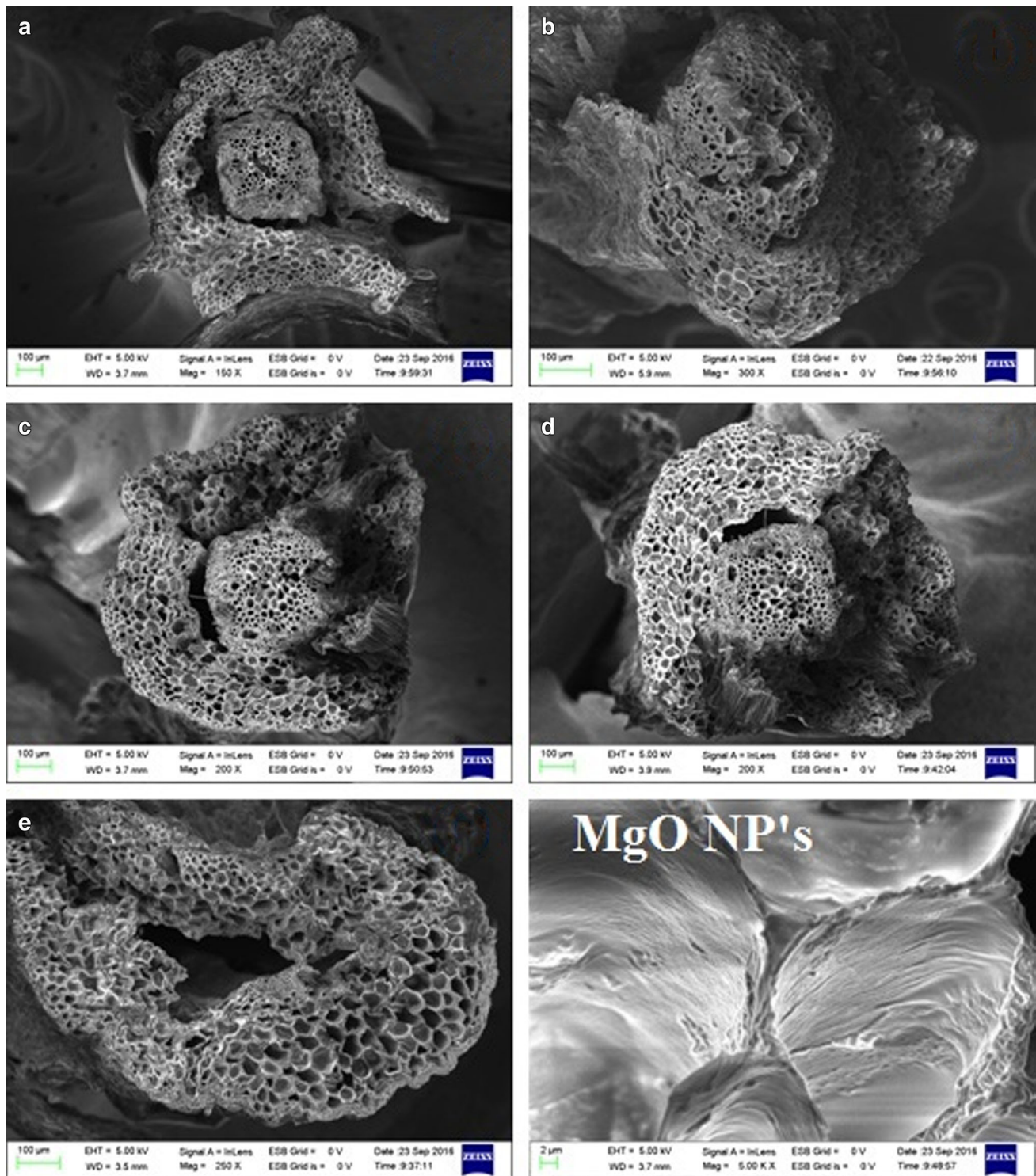
Fig. 10 SEM analyses of MgO NPs **a** 20 nm, **b** 18.5 nm, **c** 18 nm, **d** 16.5 nm, and **e** 15 nm with treated peanuts

showed enhanced chlorophyll in peanut leaves. The reason clearly demonstrates that the superior improvement in seed germination, biomass, dry biomass, and chlorophyll (photosynthetic) pigment by the application of biosynthesized MgO NPs at different sizes. Mg involves in photosynthesis,

respiration, and biosynthesis mechanism of phytohormones, and chlorophyll also involves in electron transfer redox reactions (Kim et al. 2014; Xu et al. 2015). The present results confirm that the addition of MgO NPs suspension to seeds increases the seed germination, biomass,

and chlorophyll content in the peanut plants. Finally, the MgO NPs were notably increased peanut growth in terms of seed germination, biomass, and chlorophyll content (Fig. 9).

SEM analyses of peanut plant roots

The aim of the present work is to analyze the penetration and movement of NPS in plant cells through SEM studies. No remarkable NP depositions have been observed in the root cells even after the application carried out 6 days after the suspension. At the same time in case of MgO NPs, the large number of suspended particles accumulated on roof surfaces (Fig. 10), it is clear that those MgO NPs were taken up by the peanut plants and moved into various tissues (Chsistian et al. 2012; Zhu et al. 2008). In SEM studies, we observed that the strongest magnification (5.00 kx) right above the roots may be due to NP agglomeration. All the different sizes of MgO NP samples showed greater performance than control sample. The root analysis results demonstrate that 16.5 and 15 nm-sized MgO NPs (0.5 mg/L) were be utilized to simulate the root development of peanut plants under specific conditions. From these observations, MgO NPs will be useful to stimulate seed germination and the growth of peanut plants.

Conclusion

Magnesium oxide NPs were successfully synthesized and which is confirmed by XRD and EDS. From XRD analysis, the average crystallite sizes were calculated (20, 18.5, 18, 16.5, and 15 nm), which were exactly correlated with the particle size histograms (PSA). SEM confirmed the surface morphology and size of the synthesized NPs. The elemental composition confirmed by EDS. The weight losses of MgO NPs were investigated by TG/DTA. The results demonstrate that the crystalline size decreased and then the seed germination was increased by penetrate into seed coat and supports water uptake inside seeds (Khodakovskaya et al. 2009) This activated water uptake process could be responsible for the significantly faster germination rates and higher biomass production for the plants that were exposed to small sized 16.5 and 15 nm of MgO NPs (0.5 mg/L). Molecular mechanisms of MgO induced water uptake inside plants seeds are not clear and require further investigation. The MgO NPs have positive effect on the seed germination, chlorophyll affect on peanut plants could have significant economic importance in agriculture related sector.

References

Anthony KJP, Murugan M, Jeyaraj M, Rathinam NK, Sangiliyandi G (2014) Synthesis of silver nanoparticles using pine mushroom extract: a potential antimicrobial agent against *E. coli* and *B. subtilis*. J Ind Eng Chem 20:2325–2331

Bar H, Bhui DK, Sahoo GP, Sarkar P, Pyne S, Misra A (2009) Green synthesis of silver nanoparticles using seed extract of *Jatropha curcas*. Colloids Surf Physiochem Eng Aspects 348:212–216

Chsistian O, Dimkpa Joan E, McLean Drew E et al (2012) CuO and ZnO nanoparticles: phytotoxicity, metal speciation, and induction of oxidative stress in sand-grown wheat. J Nanopart Res 14:1125

Ganesan V, Devi JA, Astalakshmi A, Nima P, Thangaraja A (2013) Eco-friendly synthesis of silver nanoparticles using a sea weed, *Kappaphycus alavarezii*. Int J Eng Adv Technol 2:559–563

Hayashi H, Hakuta Y (2010) Hydrothermal synthesis of metal oxide nanoparticles in supercritical water. Materials 3:3794–3817

Hou Y, Yu J, Gao S (2003) Solvothermal Reduction synthesis and characterization of superparamagnetic magnetite nanoparticles. R Sco Chem J Mater Chem 13:1983–1987

Jaison J, Chan YS, Michael K (2017) Danquah biosynthesis and characterization of MgO nanoparticles from plant extracts via induced molecular nucleation. New J Chem 41:2800–2814

Khodakovskaya M, Dervishi E, Mahmood M, Xu Y, Li ZR, Watanabe F, Biris AS (2009) Carbon nanotubes are able to penetrate plant seed coat and dramatically affect seed germination and plant growth. ACS Nano 3:3221–3227

Kim JH, Lee Y, Kim EJ, Gu S, Sohn EJ, Seo YS (2014) Exposure of iron nanoparticles to *Arabidopsis thaliana* enhances root elongation by triggering cell wall loosening. Environ Sci Technol 48:3477–3485

Li X, Xu H, Chen ZS, Chen G (2011) Biosynthesis of nanoparticles by microorganisms and their applications. J Nanomater 2011: (**Article ID 270974**). doi:10.1155/2011/270974

Mageshwari K, Sawanta Mali S, Sathyamoorthy R, Patil PS (2013) Template-free synthesis of MgO nanoparticles for effective photocatalytic applications. Powder Technol 249:456–462

Matteis LD, Custardoy LC, Pacheco F, Magen C, Jesus M, Fuente DL, Marquina C, Ibarra MR (2012) Ultrathin MgO coating of superparamagnetic magnetite nanoparticles by combined coprecipitation and sol-gel synthesis. Chem Mater 24:451–456

Mirzaei H, Davoodnia A (2012) Microwave assisted sol-gel synthesis of MgO nanoparticles and their catalytic activity in the synthesis of Hantzsch 1, 4-dihydropyridines. Chin J Catal 33:1502–1507

Panigrahi S, Kundu S, Ghosh SK, Nath S, Pal T (2004) General method of synthesis for metal nanoparticles. J Nanopart Res 6:411–414

Patil AB, Bhanage BM (2013) Novel and green approach for the nano crystalline magnesium oxide synthesis and its catalytic performance in Claisen–Schmidt condensation. Catal Commun 36:79–83

Ramesh R, Tarafdar JC, Singh SK, Gautam R, Choudhary K, Maurino VG, Saharan V (2014) MgO nanoparticles biosynthesis and its effect on chlorophyll contents in the leaves of Clusterbean (*Cyamopsis tetragonoloba* L.). Adv. Sci. Eng. Med 6:538–545

Sachin S, Anupama P, Meenal K (2012) Biosynthesis of silver nanoparticles by marine bacterium, idiomarine Sp. PR-58-5. J Bull Mater Sci 35:1201–1205

Sadeghi M, Hosseini M (2012) Nucleophilic Chemistry of the synthesized magnesium oxide (Magnesia) nanoparticles via microwave@sol-gel process for removal of sulfurous pollutant. Int J BioInorg Hybd Nanomat 1:175–182

Saifuddin N, Wong CW, Yasimura AN (2009) Rapid Biosynthesis of silver nanoparticles using culture supernatant of bacterial with microwave irradiation. E J Chem 6:61–70

Sushma NJ, Prathyusha D, Swathi G, Madhavi T, Raju BDP, Mallikarjuna K, Kim HS (2016) Facile approach to synthesize magnesium oxide nanoparticles by using *Clitoria ternatea* characterization and in vitro antioxidant studies. Appl. Nanosci 6:437–444

Sutradhar N, Sinhamahapatra A, Sandip PK, Pal P, Bajaj CH, Mukhopadhyay I, Panda AB (2011) Controlled synthesis of different morphologies of MgO and their use as solid base catalysts. J Phys Chem C 115:12308–12316

Tamilselvi P, Yelilarasi A, Hema M, Anbarasan R (2013) Synthesis of hierarchical structured MgO by sol-gel method. Nano Bull 2:130106

Thakkar KN, Mhatre SS, Parikh RY (2010) Biological synthesis of metallic nanoparticles. Nanomedicine 6:257–262

Vatsha B, Tetyana P, Shumbula PM, Ngila JC, Sikhwivhil LM, Moutloali RM (2013) Effects of precipitation temperature on nanoparticle surface area and antibacterial behaviour of Mg(OH)2 and MgO nanoparticles. J Biomateri Nanobiotechnol 4:365–373

Xu LH, Patil DS, Yang J, Xiao J (2015) Metal oxide nanostructures: synthesis, properties, and applications. J Nanotechnol 2015: (**Article ID 135715**). doi:10.1155/2015/135715

Yang Q, Sha J, Wang L, Yang D (2006) MgO nanostructures synthesized by thermal evaporation. Mater Sci Eng C 26:1097–1101

Zhang XF, Lic ZG, Shen W, Gurunathan S (2016) Silver nanoparticles: synthesis, Characterization, properties, applications and therapeutic approaches. Int J Mol Sci 17:1501–1534

Zhu H, Han J, Xiao JQ, Jin Y (2008) Uptake, translocation, and accumulation of manufactured iron oxide. J Environ Monit 10(6):713–717. doi:10.1039/b805998e.